J|A|C|S
ARTICLES

Published on Web 05/22/2009

Quantum Dots As Ultrasensitive Nanoactuators and Sensors of Amyloid Aggregation in Live Cells

M. Julia Roberti,[†,‡] Marcos Morgan,[§] Guillermo Menéndez,[†] Lía I. Pietrasanta,[§] Thomas M. Jovin,[‡] and Elizabeth A. Jares-Erijman*[,†]

Departamento de Química Orgánica, Facultad de Ciencias Exactas y Naturales (FCEyN), Universidad de Buenos Aires (UBA), CIHIDECAR, CONICET, Buenos Aires, Argentina, Laboratory of Cellular Dynamics, Max Planck Institute for Biophysical Chemistry, Göttingen, Germany, DFG Forschungszentrum CMPB "Molecular Physiology of the Brain", Göttingen, Germany, Laboratorio Max Planck de Dinámica Celular, FCEyN, UBA, Buenos Aires, Argentina, and Centro de Microscopías Avanzadas, CONICET, FCEyN, UBA, Buenos Aires, Argentina

Received January 12, 2009; E-mail: eli@qo.fcen.uba.ar

Abstract: Quantum dots multifunctionalized with the amyloid protein α-synuclein act at nanomolar concentrations as very potent inducers of the aggregation of micromolar−millimolar bulk concentrations of the protein *in vitro* and in cells. Fibrillation in live cells, a process diagnostic of Parkinson's disease, is accelerated up to 15-fold with only ∼100 nanoparticles. The combination with a tetracysteine-tagged form of α-synuclein specific for fluorogenic biarsenicals constitutes a very sensitive system for studying pathological amyloid formation in cells.

Introduction

Fluorescent probes in live-cell imaging are fundamental tools for assessing cellular function.[1,2] They include quantum dots (QDs), fluorescent semiconductor nanoparticles whose burgeoning impact on cellular biology[3] and bioanalytics[4,5] is comparable to that of visible fluorescent proteins. This circumstance is due to their exceptional photostability, broad excitation, narrow tunable emission, single molecule detectability,[6] and suitability for multiplexing.[5,7] A novel intriguing potential for these and related nanoparticles, however, lies in their capacity for functioning as specific "nanoactuators", i.e., as active reagents. In this report, we demonstrate that smart-tailored QDs can induce the controlled generation of desired cellular responses. We assembled artificial centers for the nucleation of the amyloid aggregation of the protein α-synuclein (AS), using streptavidin-coated QDs loaded with biotinylated AS. These specific seeds promoted the aggregation of AS both *in vitro* and in live cells in a controlled fashion.

AS is an abundant and natively unstructured presynaptic protein (140 aa).[8] Aberrant, amyloid fibrillar deposits of this protein are characteristic features in the brains of patients suffering from Parkinson's disease and other neurodegenerative diseases classified as synucleinopathies.[8,9] Cytotoxicity is attributed to as yet poorly defined oligomeric intermediates species in the aggregation pathway,[10] the study of which has been hampered by a dearth of suitable expression systems. We recently introduced a recombinant AS (AS-C4)[11] bearing a tetracysteine motif as an expression tag.[2] AS-C4 binds biarsenicals such as FlAsH to produce highly fluorescent adducts (AS-C4-FlAsH) retaining the biophysical, biochemical, and aggregation properties of wild-type AS *in vitro* and in cells.[11]

The mechanisms underlying the physiological function of AS and the conditions leading to its pathological self-association are still unclear.[12] Cellular studies of amyloid aggregation often incorporate chemically induced oxidative stress[13] as a triggering mechanism; as a consequence complex secondary effects are inevitable. The simultaneous application of the AS-C4 system and the QD reagents featured here offers very high specificity,

[†] Departamento de Química Orgánica, UBA.
[‡] Max Planck Institute for Biophysical Chemistry, DFG Forschungszentrum CMPB "Molecular Physiology of the Brain", and Laboratorio Max Planck de Dinámica Celular, UBA.
[§] Centro de Microscopías Avanzadas, UBA.

(1) O'Hare, H. M.; Johnsson, K.; Gautier, A. *Curr. Opin. Struct. Biol.* **2007**, *17*, 488–494.
(2) Soh, N. *Sensors* **2008**, *8*, 1004–1024.
(3) (a) Alivisatos, A. P.; Gu, W.; Larabell, C. *Annu. Rev. Biomed. Eng.* **2005**, *7*, 55–76. (b) Pinaud, F.; Michalet, X.; Bentolila, L. A.; Tsay, J. M.; Doose, S.; Li, J. J.; Iyer, G.; Weiss, S. *Biomaterials* **2006**, *27*, 1679–1687.
(4) Lin, C. A. J.; Liedl, T.; Sperling, R. A.; Fernández-Argüelles, M. T.; Costa-Fernández, J. M.; Pereiro, R.; Sanz-Medel, A.; Chang, W. H.; Parak, W. J. *J. Mater. Chem.* **2007**, *17*, 1343–1346.
(5) Susumu, K.; Uyeda, H. T.; Medintz, I. L.; Pons, T.; Delehanty, J. B.; Mattoussi, H. *J. Am. Chem. Soc.* **2007**, *129*, 13987–13996.
(6) Zhang, C. Y.; Johnson, L. W. *J. Am. Chem. Soc.* **2008**, *130*, 3750–3751.
(7) (a) Eastman, P. S.; Ruan, W.; Doctolero, M.; Nuttall, R.; de Feo, G.; Park, J. S.; Chu, J. S.; Cooke, P.; Gray, J. W.; Li, S.; Chen, F. F. *Nano Lett.* **2006**, *6*, 1059–1064. (b) Liu, W.; Howarth, M.; Greytak, A. B.; Zheng, Y.; Nocera, D. G.; Ting, A. Y.; Bawendi, M. G. *J. Am. Chem. Soc.* **2008**, *130*, 1274–1284.
(8) Uversky, V. N. *J. Neurochem.* **2007**, *103*, 17–37.
(9) Hamley, I. W. *Angew. Chem., Int. Ed.* **2007**, *46*, 8128–8147.
(10) Waxman, E. A.; Giasson, B. I. *Biochim. Biophys. Acta*, in press (doi: 10.1016/j.bbadis.2008.09.013).
(11) Roberti, M. J.; Bertoncini, C. W.; Klement, R.; Jares-Erijman, E. A.; Jovin, T. M. *Nat. Methods* **2007**, *4*, 345–351.
(12) Lansbury, P. T.; Lashuel, H. A. *Nature* **2006**, *443*, 774–779.
(13) (a) Ebadi, M.; Sharma, S. K.; Ghafourifar, P.; Brown-Borg, H.; El Refaey, H. *Methods Enzymol.* **2005**, *396*, 276–298. (b) Lev, N.; Melamed, E.; Offen, D. *Neurosci. Lett.* **2006**, *399*, 27–32.

10.1021/ja900225w CCC: $40.75

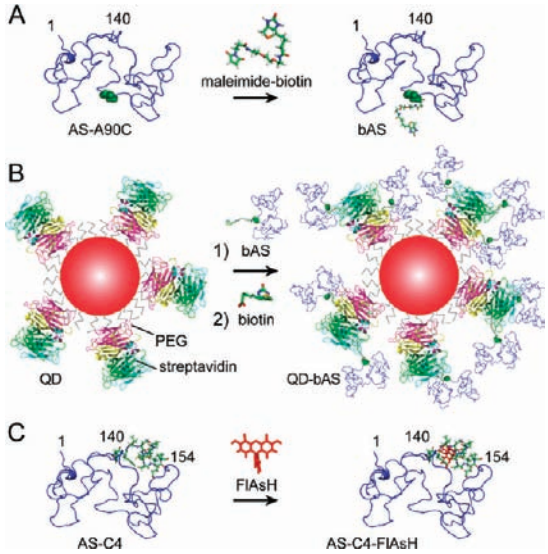

Figure 1. Strategy for QD-induced aggregation of AS. (A) AS containing an A90C point mutation (AS-A90C) was biotinylated (bAS) for binding to streptavidin-functionalized QD605. (B) The artificial seeds for aggregation were assembled by incubation of QDs with bAS (step 1) and blocking remaining binding sites with biotin (step 2). Different QD/bAS molar ratios were assayed to evaluate the effect of the bAS loading on the ability of QD-bAS to function as nuclei for aggregation. (C) AS with an engineered tetracysteine tag (AS-C4) that complexes fluorogenic biarsenical compounds (e.g., FlAsH) was used as the bulk protein for aggregation assays. QD-bAS were incorporated in 100 μM solutions of AS-C4 protein for aggregation assays *in vitro* or in 100 μM solutions of AS-C4-FlAsH for microinjection into live HeLa cells. The nanoparticle concentrations were $<10^{-5}$ that of the bulk protein. AS cartoons were adapted from previous models.[27] The structure of streptavidin was obtained from the Protein Data Bank, http://www.pdb.org.

no known side effects, and optimal high resolution imaging of accelerated protein aggregation in live cells.

Results

Generation of QD-Based Nucleation Centers. We stimulated the aggregation of AS *in vitro* and in cells with AS-conjugated QDs as nucleation seeds (Figure 1). The latter were generated by biotinylating AS containing an A90C point mutation (bAS, Figure 1A) and applying it to streptavidin-conjugated QDs (QD-bAS, Figure 1B) at various QD/bAS (1/m) ratios, thereby forming complexes with different stoichiometries. We determined that the formation of the complexes at nanomolar concentrations required incubations of at most 1 h and that they were stable (see Supporting Information). In cellular studies, QD-bAS was microinjected into HeLa cells together with an $\sim 10^4-10^5$ excess of AS-C4-FlAsH (Figure 1C). The two fluorophores emit at 530 nm (AS-C4-FlAsH) and 605 nm (QDs) upon excitation at 480 nm (Supporting Figure S1). The net QD-bAS concentrations were <10 nM in the *in vitro* assays and $\sim 10^2$ nanoparticles per cell.

Triggering and Modulation of AS Aggregation in Vitro. The kinetics of aggregation of AS-C4 *in vitro* was monitored by a standard assay based on the fluorescence increment exhibited by ThioflavinT upon binding to β-sheet amyloid structures.[14] We assessed the function of QD-bAS in promoting AS aggregation by adding QDs loaded with bAS to different levels (m = 0, 1, 4, 8, 20, 40, 80, and 200) to the monomeric protein under normal assay conditions. The ensuing time course of aggregation was analyzed according to the following representation of the nucleation−propagation mechanism generally invoked for amyloid formation:[15,16]

$$\alpha(t) = \frac{e^{k_{app}t} - 1}{e^{k_{app}t} + e^{k_{app}t_{1/2}} - 2} \quad (1)$$

Expression 1 is obtained as the solution of the differential equation for depletion of monomeric AS, present at an initial concentration $[AS]_0$, by association with amyloid product, leading to a progressive increase of the latter from an initial concentration of nucleation centers, $[nc]_0$, presumed to form spontaneously and at very low levels from the monomeric protein. The time course for the monomer-to-fibril conversion, normalized by ($[AS]_0 - [nc]_0$), is represented by the fractional, dimensionless quantity $\alpha(t)$. The two parameters of eq 1 are $t_{1/2}$, the time required to reach the midpoint of the rapid growth phase, and an apparent growth rate constant,[17] $k_{app} = k_{agg}[AS]_0$, with k_{agg} as the second-order rate constant for incorporation of the monomer into the growing amyloid fibrils.

A substantial acceleration of aggregation was observed in the presence of QD-bAS complexes, as manifested by a progressive decrease in $t_{1/2}$ to a degree dependent on m (Figure 2A) but achieving a plateau value of ~40% for $m \geq 80$ (Figure 2A,B). The corresponding values of k_{agg} (mean value: 1.5 ± 0.5 mM^{-1} h^{-1}) did not change appreciably with m. QDs devoid of bAS or loaded with equimolar bAS (m = 0 and 1, respectively) had no perceptible effect on aggregation. A reduction in $t_{1/2}$ also occurred with increasing concentrations of QD-bAS for a fixed loading, m = 80 (Figure 2C,D). In the latter, the enhancement was significant for a QD-bAS concentration as low as ~0.2 nM, i.e., 10^5-fold lower than the concentration of monomeric AS-C4.

We performed a quantitative analysis of the kinetic data after introducing an additional term, *nef*, in the nucleation−propagation model of eq 1, recasted as an expression for $t_{1/2}$ (eqs 2 and 3).

$$t_{1/2} = \ln\left[1 + \frac{[AS]_0}{[nc]_0(1 + nef)}\right]\frac{1}{k_{app}} \quad (2)$$

$$nef = \gamma(m)[\text{QD-bAS}]_{tot} \quad (3)$$

The nucleation enhancement factor, *nef*, defined as the product of a QD-associated AS interaction parameter, $\gamma(m)$, and the total concentration of nanoparticles, is conceived as operating on the initial concentration of nucleation centers formed in the absence of QDs, $[nc]_0$, such as to increase their number by the factor *nef*. The fits to the m = 80 data at varying QD-bAS concentration (Figure 2D) yielded estimates for the parameters of eqs 1−3: $k_{agg} = 1.4 \pm 0.2$ mM^{-1} h^{-1}, $\gamma = 12 \pm 6$ nM^{-1}, and $[nc]_0 \approx 3$ nM.[18] The value of k_{agg} was in excellent agreement with direct estimations from the individual kinetic traces, 1.5 ± 0.5 mM^{-1} h^{-1} (Figure 2A; eq 1), as well as the range of elongation

(14) Celej, M. S.; Jares-Erijman, E. A.; Jovin, T. M. *Biophys. J.* **2008**, *94*, 4867–4879.

(15) (a) Wetzel, R. *Acc. Chem. Res.* **2006**, *39*, 671–9. (b) Powers, E. T.; Powers, D. L. *Biophys. J.* **2008**, *94*, 379–391.

(16) Colaco, M.; Park, J.; Blanch, H. *Biophys. Chem.* **2008**, *136*, 74–86.

(17) Fernández, C. O.; Hoyer, W.; Zweckstetter, M.; Jares-Erijman, E. A.; Subramaniam, V.; Griesinger, C.; Jovin, T. M. *EMBO J.* **2004**, *23*, 2039–2046.

(18) It is gratifying yet not intuitive that the rate constant for monomer addition to the amyloid aggregate, k_{agg}, could be determined solely from the $t_{1/2}$ values in such experiments, inasmuch as the estimation of this quantity usually requires analysis of the entire time course of aggregation, or at least of the maximal slope at the midpoint.

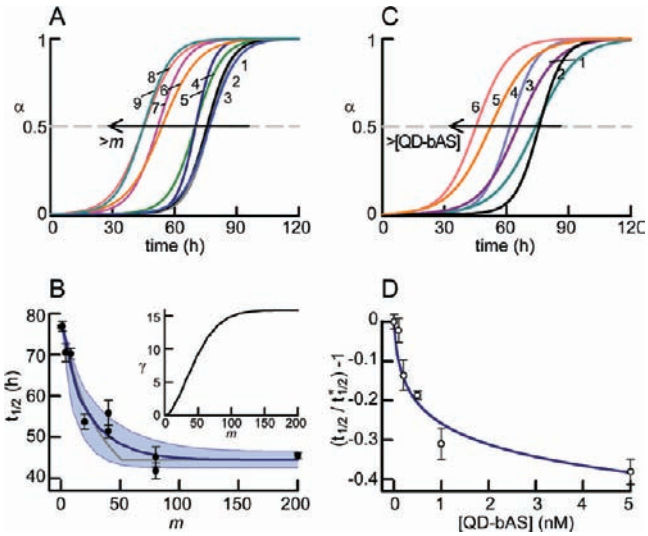

Figure 2. Effect of QD-bAS on the aggregation of AS *in vitro*. (A) Aggregation kinetic curves, generated from mean parameters derived from duplicate determinations (Supporting Information), of 100 μM AS-C4 as a function of the degree of loading of the nanoparticles with bAS, represented by m, the number of bAS molecules added per QD. Curves designated by numbers in parentheses: AS-C4 without QDs (1), AS-C4 coincubated with 5 nM QD-bAS with $m = 0$ (2), 1 (3), 4 (4), 8 (5), 20 (6), 40 (7), 80 (8), and 200 (9). (B) Dependence of $t_{1/2}$ on increasing m (0−200, black dots). Grey curve: Eqs 2−4 with $s = 4.5$, $k = 2$, $\beta = 0.35$, $[AS]_0/[nc]_0 = 100/0.003$, and $k_{agg} = 1.35$ mM^{-1} h^{-1}. Dark blue curve: Version of eq 2 with $\gamma(m) = \sum_{i=1}^{3s}(e^{-s}s^i)/(i!)\, Min[4,(\beta m)/(i)]^k$ representing a presumed Poissonian distribution of streptavidin molecules/QD with mean value s ($i = 1-3s$). Inset: $\gamma(m)$with the same parameter values as above except for $\beta = 0.25$. The shaded area encompasses curves generated with parameters $s = 4.5 \pm 0.5$, $k = 2 \pm 0.2$, and $\beta = 0.3 \pm 0.1$. Error bars here and in (D), standard errors (s.e.) of individual and pooled fits to the original aggregation curves (Figure 2A); the 95% confidence interval is conventionally given by $\pm$ 2s.e. (C) Aggregation kinetics of 100 μM AS-C4 as a function of the concentration of QD-bAS ($m = 80$): AS-C4 alone (1), AS-C4 coincubated with 0.1 nM (2), 0.2 nM (3), 0.5 nM (4), 1 nM (5), and 5 nM (6) QD-bAS. (D) Relative decrease in $t_{1/2}$ with increasing concentrations of QD-bAS ($m =$ 80, white dots). Here, $t^*_{1/2}$ denotes the half lifetime of aggregation of AS-C4 alone. Fit according to eq 2 (blue curve; Supporting Information).

rate constants recently reported for the aggregation of polyglutamine.[16] The computed parameters establish that the QD complexes are extremely effective seeds, judging from the calculation that 1 nM QDs loaded with bAS would lead to an ~10-fold increase in the nucleation of a 10^5-fold higher concentration (100 μM) of monomeric AS.

We assumed a simple phenomenological functional form for the interaction parameter γ (m):

$$\gamma(m) = \min\left[\frac{\beta m}{s}, 4\right]^k \qquad (4)$$

where β represents an empirical "loading factor" accounting for various influences acting to depress m from its nominal values (Supporting Information), and s is the average number of streptavidin molecules per QD. An independent estimation of s was performed by titrating nanoparticles preloaded with 0, 8, and 20 equiv of bAS, with a biotinylated pH indicator serving as an FRET-acceptor.[19] The resultant value, $s = 4-5$, was compatible with other reports[20] (manufacturer: 5−10).

According to the proposed function (eq 4), the binding stoichiometry of tetrameric streptavidin—given by $(\beta m)/(s)$ for values ≤4, or 4 for $(\beta m)/(s) > 4$—is raised to the power k. The latter parameter can be regarded as a *reaction order* for interaction(s) between local (corresponding to the streptavidin anchors) densities of bAS bound firmly to the nanoparticle. Note that for $k > 1$, γ is <1 for $(\beta m)/(s) < 1$; i.e., it acts to damp the QD influence, whereas, for $(\beta m)/(s) > 1$, γ increases rapidly up to the limit 4^k (Inset, Figure 2B). Under this condition, k is determined upon specification of $[AS]_0/[nc]_0$, [QD], and the plateau value of relative $t_{1/2}$.

A fit to the $t_{1/2}(m)$ data based on eqs 2−4, considering $s =$ 4.5, and $[AS]_0/[nc]_0 = 100/0.003$, yielded $k = 1.9$ and $\beta \approx 0.3$. Parameter variation (Figure 2B) led to a zone of acceptable solutions regardless of whether a fixed or a distribution value of s was assumed. We interpret the value of k close to the integer 2 as an indication for a structure of the QD-bAS complex facilitating AS dimerization as an event conducive to nucleation. The existence of a dimer was inferred previously from our biochemical and NMR studies of polyamine-AS complexes.[17]

We also explored an alternative model attributing the nucleation enhancement of QD-bAS to the concerted behavior of bAS molecules bound to individual albeit noninteracting streptavidin molecules. The best fit to the data required larger values of s and the assumption that only fully saturated streptavidins were competent in nucleation. Such a model implies that complexes of free streptavidin and bAS in solution, i.e., in the absence of nanoparticles, should be equally effective. However aggregation assays performed with up to 50 nM streptavidin fully loaded with bAS led to a <10% decrease in $t_{1/2}$. We conclude that collective interactions promoted by the s streptavidin molecules acting in concert with particular surface characteristics of the QD nanoparticles are required for the efficient nucleation of bulk AS aggregation.

Imaging Nanoactuator−Protein Interactions at the Single Particle Level by Fluorescence Microscopy and AFM. The aggregates generated in the presence of QD-bAS were examined by fluorescence microscopy to establish whether the nanoparticles were being incorporated. The products formed from mixtures of AS-C4 and QD-bAS ($m = 0$, 1, and 40) were labeled with FlAsH and imaged with two-channel detection (Figure 3). For $m = 40$, QDs incorporated into the fibrillar mesh (Figure 3A,B), whereas AS-C4 aggregates generated in the presence of QD-bAS, $m = 0$, 1, were devoid of QDs (Supporting Figure S2). The morphology was the same in all cases (Figure 3A−C), and the amyloid nature of the samples was confirmed by ThioflavinT staining (Supporting Figure S3). We used different contrast modes of atomic force microscopy (AFM) to visualize the interactions between QDs and AS fibrils at high spatial resolution (Figure 3 D,E; Supporting Figure S4). QD-bAS complexes were observed in close association with fibrils, for $m = 40$ (Figure 3D−F) but not for $m = 0$, 1 (Supporting Figure S4). The fibrillar structural features matched those of AS aggregated in the absence of QDs (Figure 3G).

QDs as Nanoactuators of Amyloid Formation in Live Cells. The most dramatic effects of QD-bAS were achieved in investigations of AS aggregation in live cells. We modified protocols established in our prior studies of AS-C4-FlAsH (100 μM) microinjected into HeLa cells[11] by inclusion of 5 nM QD-bAS with $m = 0$, 1, 8, and 80, with the labeled protein. The estimated dilution upon delivery into the cells was ~10-fold, leading to an estimated 10 μM of AS-C4-FlAsH and 100−300 QDs, initially distributed uniformly in the cytoplasm. The cells

(19) Menéndez, G.; Roberti, M. J.; Sigot, V.; Etchehon, M.; Jovin, T. M.; Jares-Erijman, E. A. *Proc. SPIE* **2009**, *7189*, 71890P1–71890P9.
(20) Swift, J. L.; Heuff, R.; Cramb, D. T. *Biophys. J.* **2006**, *90*, 1396–1410.

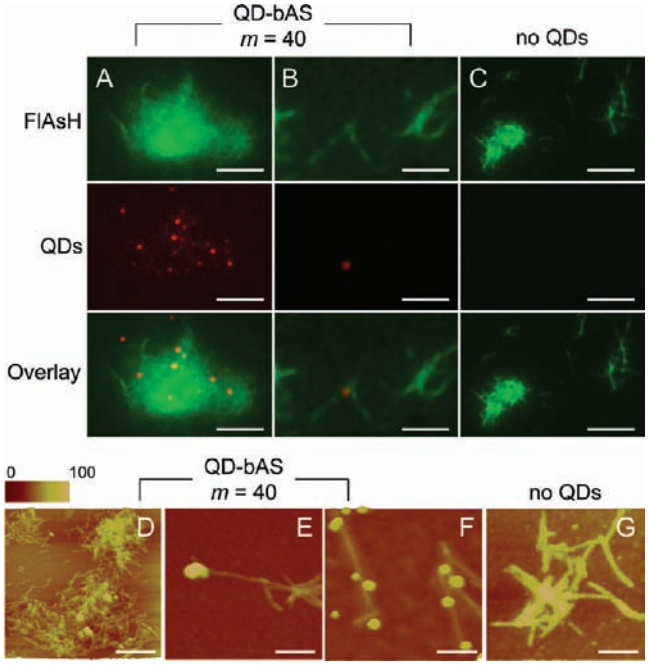

Figure 3. Optical and AFM imaging of *in vitro* AS/QD-bAS interactions in amyloid aggregates. Fluorescence microscopy images of aggregates and fibrils prepared from (A, B) AS-C4 coincubated with QD-bAS, $m = 40$, and (C) AS-C4 alone. The samples were labeled with FlAsH, purified by centrifugation and spin-coated onto glass coverslips in PBS buffer with 1% PVA. Scale bars: (A, C) 10 μm, (B) 5 μm. The nature of the interaction was further investigated by AFM. In this case we used AS instead of AS-C4-FlAsH, as AFM does not require labeled protein and AS and AS-C4-FlAsH have matching biophysical and biochemical properties.[11] (D, E, F) Fibrils obtained from mixtures of AS and QD-bAS $m = 40$, and (G) AS alone, deposited on freshly cleaved mica and visualized in tapping mode AFM. Surface plots at 0° viewing angle to emphasize topography. Scale bars: (A, C, D, E, F, G) 10 μm; (B) 5 μm. Height in nm indicated by the colored scale bar.

were imaged 24 h (and 48 h in the case of AS-C4-FlAsH alone) after microinjection (Figure 4), and the efficiency of aggregation was estimated from the relative projected intensity and area of AS-C4-FlAsH aggregates, determined as follows. A mask, M_{cell}, was generated for each cell from the AS-C4-FlAsH fluorescence signal, and the total area, A_{cell}, and fluorescence intensity, I_{cell}, were calculated. A mask for AS-C4-FlAsH aggregates, M_{agg}, was established using the mean + 5 × s.d. (standard deviation) of AS-C4-FlAsH intensity in a region devoid of aggregates as a threshold, leading to determinations of total area, A_{agg}, and fluorescence intensity, I_{agg}, in the aggregates, and the corresponding percentile fractions of aggregated area, $100 \cdot A_{agg}/A_{cell}$, and intensity, $100 \cdot I_{agg}/I_{cell}$.

In these procedures, the microinjected QDs were readily detected and localized (Figure 4A). However, aggregation of AS-C4-FlAsH was virtually undetectable at 24 h in cells lacking QD-bAS (Figure 4B) or microinjected with unloaded QDs (Figure 4C); quantitative evaluation yielded estimates of 1−2% aggregation (Figure 4G and Supporting Table T1). In the case of microinjected QD-bAS, incipient deposits were weakly apparent for $m = 1$ (Figure 4D), and to a very significant degree with $m = 8$ (Figure 4E), and $m = 80$ (Figure 4F) at 24 h. The calculations based on the intensities and areas of the aggregates indicated a ∼2-, 10-, and 15-fold increase for $m = 1$, 8, and 80, respectively, relative to the cells microinjected with AS-C4-FlAsH alone or with nonloaded QDs (Figure 4G and Supporting Table T1). An alternative formulation of the results is to note that the fully loaded QD-bAS, present at nanomolar levels, induced the aggregation of an ∼4000-fold higher relative concentration of monomeric AS. In the absence of QDs, only ∼10% of the AS-C4-FlAsH was aggregated at the 48 h time point (Figure 4H). An interesting additional finding was a significant sensitization of QD emission in the presence of aggregated AS-C4-FlAsH (QD channel in Figure 4), indicative of a potential intervention of one or more FRET processes (see Discussion).

Discussion and Conclusions

The procedures featured in this report provide very simple and useful tools for inducing and evaluating amyloid aggregation in live cells, which exhibited interesting correlations with the experiments *in vitro*. In both situations, the addition of QD-bAS led to an acceleration of AS aggregation to a degree dependent on the loading level of the nanoparticles (Figures 2B, 4G). The effects were already significant for concentrations of saturated QD-bAS as low as ∼0.2 nM (Figure 2D). The close association of the nanoparticles with the aggregates was revealed by fluorescence microscopy demonstrating colocalization of the fluorescence signals of bulk protein and the QD seeds and by AFM *in vitro*. Furthermore, the observed blinking of the QDs, a phenomenon generally considered as indicative of individual nanoparticles, established that the induced aggregation was not the consequence of extensive clustering of multiple nucleation centers (Supporting Figure S5 and Supporting Movie M1).

The significant aggregation enhancement observed in live cells suggests that the intracellular QD-bAS complexes do not dissipate, i.e., by progressive dissociation of the bAS[20] promoted by excess biotin added as a suppressor of nonspecific intracellular binding. As stated above for the samples *in vitro*, the nucleation centers were also effective in the cellular environment at very low concentrations. We conclude that nucleation ensued fairly rapidly either after introduction of QD-bAS into high concentrations of AS *in vitro* and exposure to elevated temperature or after loading into cells. Stabilization presumably arises from multiple, cooperative molecular interactions involving numerous AS molecules bound to a given QD and, progressively, in solution.

We would emphasize the extreme sensitivity of the technique featured in this report for promoting and detecting the aggregation of the amyloid protein AS. Our experiments were conducted under physiological conditions and with low nanoparticle concentrations (≤5 nM). The QDs were inactive in the absence of specifically bound AS molecules, thus exhibiting a selectivity not displayed by nanostructures employed at much higher concentrations.[21] Furthermore, QD-bAS functioned in the cells as efficient scaffolds for nucleation capable of targeting the fluorescently labeled AS molecules in the complex, crowded cellular milieu. They also exhibited an enhanced emission, possibly reflecting their association with the target protein AS-C4-FlAsH serving as a donor for cascaded homotransfer−heterotransfer FRET processes. Evidence for such a phenomenon was provided[22] by "k_t/k_f" images[23] generated according to a new FRET formalism.[24] The aggregates of the FlAsH

(21) Linse, S.; Cabaleiro-Lago, C.; Xue, W. F.; Lynch, I.; Lindman, S.; Thulin, E.; Radford, S. E.; Dawson, K. A. *Proc. Natl. Acad. Sci. U.S.A.* **2007**, *104*, 8691–8696.
(22) Roberti, M. J.; Jovin, T. M.; Jares-Erijman, E. A. Manuscript in preparation.
(23) k_t, rate constant for FRET; k_f, radiative rate constant.
(24) Jares-Erijman, E. A.; Jovin, T. M. In *FRET and FLIM Imaging Techniques*; Gadella, T., Jr., Ed.; Elsevier: 2009; pp 475−517.

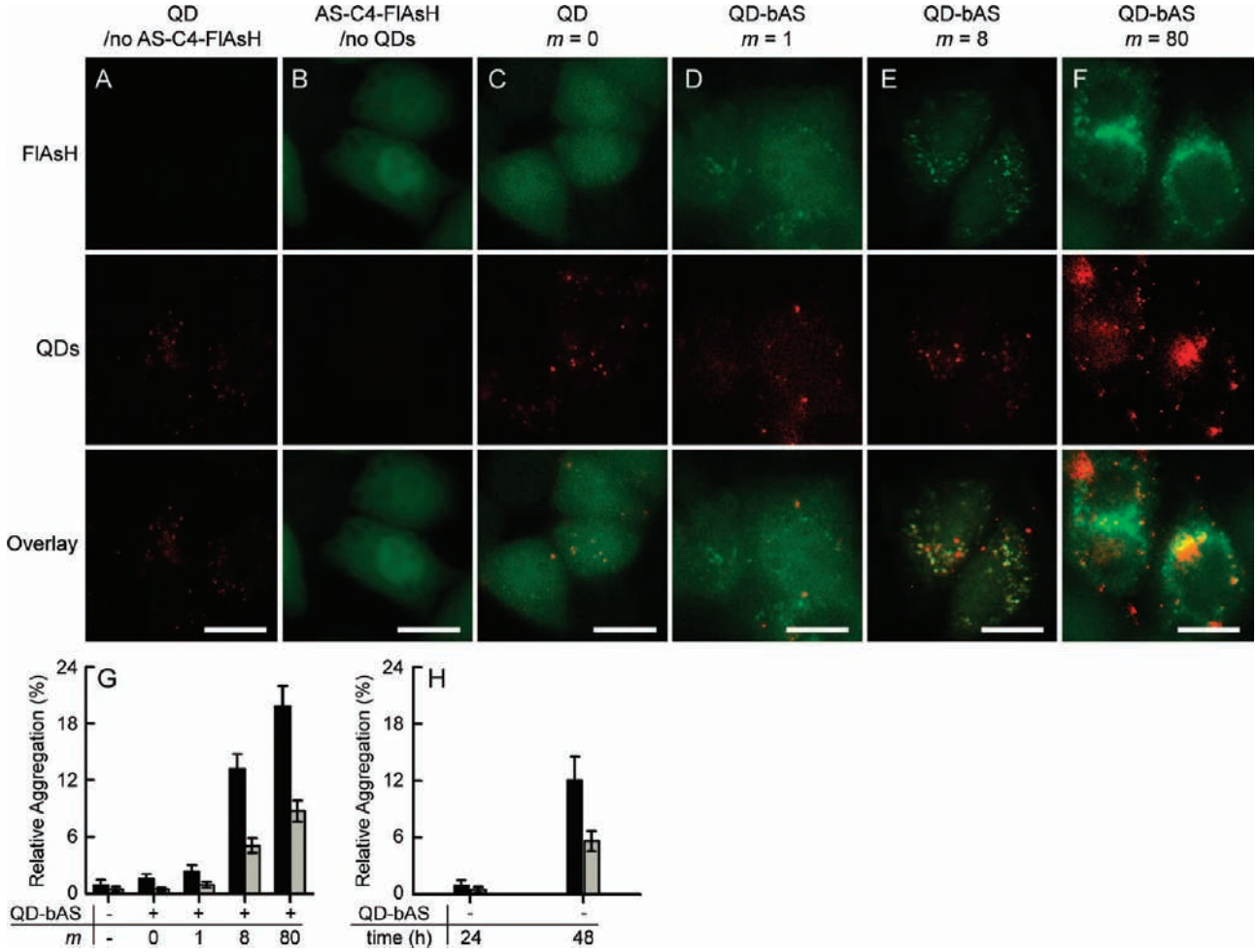

Figure 4. Induction of AS aggregation in cells by bAS-functionalized QDs. Fluorescence microscopy of HeLa cells ($\lambda_{exc} = 480$ nm), 24 h after microinjection with (A) 5 nM QDs alone, (B) 100 μM AS-C4-FlAsH, and with mixtures of 100 μM AS-C4-FlAsH and 5 nM QD-bAS at QD/bAS ratios given by (C) $m = 0$, (D) $m = 1$, (E) $m = 8$, and (F) $m = 80$. The panels display FlAsH fluorescence (top), QD emission (middle), and the colocalization of both signals (bottom). The images are representative of $n > 10$ repeats in all cases. Scale bars, 50 μm. (G) Quantitative analysis of the degree of aggregation, relative to total microinjected AS-C4-FlAsH per cell. The fraction of protein forming aggregates was estimated from the relative intensity of AS-C4-FlAsH fluorescence in aggregates (black bars) and the relative areas occupied by such structures (gray bars). See Supporting Table T1. (H) Same analysis, showing the magnitude of aggregation of AS-C4-FlAsH alone 48 h after microinjection.

labeled AS-C4 construct feature efficient energy transfer between the constituent molecules of the fibrillar amyloid structures[11] and, thus, could serve as a "donor umbrella".

In this report we have shown that the application of very low concentrations of multivalent QDs covered with AS ligands provides the conditions for the acceleration of aggregation of a much higher concentration of the same protein, probably through self-assembly of the protein initiated by the high local concentrations displayed at the surface of the nanoparticles. The system is deterministic in the sense of comprising well-defined entities and concentrations, as opposed to the use of irreproducible macerated amyloid fibrils in conventional seeding experiments. We anticipate that such QD ligands will provide important new insights into the mechanisms of oligomerization and fibrillation by identifying specific cellular organelles and compartments in which the molecular processes underlying cytotoxicity are operative. Multiplexed sensors−nanoactuators will be of particular value since proteins and cellular structures involved in amyloid-based neurodegeneration most often act in concert.[25]

Clearly, the approach featured in this report with α-synuclein should be transferable to the general family of amyloid proteins and their associated protein cofactors, e.g., Aβ and tau characteristic of Alzheimer's disease.

The design of artificial centers for nucleation can also be generalized to include functionalization of QDs with molecular species such as peptides and inhibitors, thereby impacting the fields of drug screening and therapeutics. Finally, due to their inherent nature QDs will permit single-molecule (nanoparticle) measurements in real time, particularly during the experimentally challenging first stages of oligomerization.

Experimental Section

Reagents. All reagents were of analytical grade. Qdot605-streptavidin conjugate was from Invitrogen.

Preparation of Biotinylated AS and QD-bAS. Monobiotinylated AS (bAS) was prepared as described in the literature[26] with

(25) (a) Cooper, A. A.; et al. *Science* **2006**, *313*, 324–8. (b) van Rooijen, B. D.; Claessens, M. M. A. E.; Subramaniam, V. *Biochim. Biophys. Acta*, in press (doi:10.1016/j.bbamem.2009.03.010).

(26) Hermanson, G. T. *Bioconjugate techniques*; Academic Press: San Diego; London, 1996.

(27) Bertoncini, C. W.; Jung, Y. S.; Fernandez, C. O.; Hoyer, W.; Griesinger, C.; Jovin, T. M.; Zweckstetter, M. *Proc. Natl. Acad. Sci. U.S.A.* **2005**, *102*, 1430–5.

slight modifications. The stock solution (~700 μM) of AS carrying an A90C point mutation was incubated for 15 min with fresh 2 mM DTT to reduce disulfide bonds. DTT was removed using a PD10 column (GE Healthcare). A 500 μL aliquot of 300 μM protein in 20 mM Na-Hepes, pH 7.2, 1 mM TCEP, was incubated for 4 h at room temperature with a 15-fold molar excess of the biotin maleimide reagent (EZ-link PEG2 biotin maleimide, Pierce). The sample was purified on a PD-10 column (Biorad), and dialyzed against 20 mM Hepes buffer, 1 mM DTT for 72 h, changing the buffer once daily. The biotin content was determined using a standard Haba-avidin assay (Sigma; see below). The labeling efficiency was ~55%.

For QD labeling, we incubated 20 nM QD605-streptavidin conjugate from Invitrogen, abbreviated as QD in this report, with different stoichiometric ratios of bAS (m = 1, 4, 8, 20, 40, 80, and 200) in PBS/1% BSA buffer, for 1 h at 4 °C. A 100-fold excess biotin was then added to block residual free binding sites.

Spectroscopic Measurements. Absorption measurements were performed on a Cary 100 spectrophotometer (Varian). The AS and AS-C4 concentrations were determined by A_{275} (ϵ_{275} = 5600 M^{-1} cm^{-1}). Haba-avidin measurements to determine the biotin content in bAS were performed following the decrease in the absorbance signal at 400 nm of standard samples containing 50, 100, 150, and 200 μM biotin, and a calibration curve was constructed with these values. Steady-state fluorescent measurements were performed on a Cary Eclipse spectrofluorimeter (Varian). ThioflavinT determinations were carried out with excitation at 446 nm and detection at 480 nm. FlAsH and QD spectra (Supporting Figure S1) were measured with excitation at 480 nm.

In Vitro Aggregation Assays. Samples containing 500 μL of 100 μM AS-C4 in 20 mM Na-Hepes buffer, pH 7.2, 1 mM DTT, were incubated at 37 °C in glass vials with continuous magnetic stirring. Fibrillation was first carried out at a fixed 5 nM QD-bAS nanoparticle concentration with different degrees of nominal bAS coverage (m = 0, 1, 4, 8, 20, 40, 80, 200). Controls with AS-C4 alone were also prepared. Aggregation assays with varying QD-bAS, m = 80, concentrations (0.1, 0.2, 0.5, 1, and 5 nM) were then performed. The increase in ThioflavinT fluorescence was recorded from 5 μL aliquots withdrawn sequentially at different time points and diluted to 2 mL in 5 μM ThioflavinT, 20 mM Na-glycine buffer, pH 8. Individual fits to duplicate kinetic traces were combined to form the curves of Figure 2A using mean parameters computed as follows. Equation 1 was inverted to generate a function for the dependence of the reaction time on the progress parameter α and the fit parameters. The average of the two times calculated for $\alpha = 0.5$ was designated as the mean $t_{1/2}$ for the experiment. An average time was then computed for $\alpha = 0.95$ and introduced into the equation together with the mean $t_{1/2}$ and the desired mean k_{app}. The difference between 0.95 and eq 1 was minimized, yielding the value for k_{app}. An example of this procedure is given in Supporting Figure S6. Fits were performed with KaleidaGraph (Synergy Software) and Mathematica (Wolfram Research).

Fluorescence Microscopy. Conventional epifluorescence microscopy was carried out with an Olympus IX71 microscope equipped with an UPlanApo 60× 1.2 NA water immersion objective. FlAsH was detected with an FITC set (ex 480/30 BP, 505 DM, em 535/40 BP), and QDs 605 with a QDs 605 set (ex 480/30 BP, 590 DM, em 605/10 QDot filter) (all filters from Chroma). An image splitter equipped with a dichroic mirror (590 DM) was used to image simultaneously the FlAsH and QDs 605 channel, and the detection was achieved with an iXon emCCD camera (Andor). Image processing was performed with DIPimage toolbox for Matlab (TU Delft, Holland) and ImageJ (http://rsb.info.nih.gov).

Experiments with Live HeLa Cells. HeLa cells were cultured on CellLocate coverslips (Eppendorf) in DMEM containing 4.5 g/L glucose, 10% fetal calf serum, and 1% penicillin/streptomycin (complete medium). We microinjected the cells in serum-free medium Opti-MEM (Invitrogen) as described elsewhere,[11] using a semiautomatic microinjection apparatus and Femtotips (Eppendorf). The number of QDs per cell (~10^2) was estimated by assuming a 10-fold dilution (according to the device manufacturer's guidelines) of 5 nM QD in a cell with a volume of 1 pL.

Quantitative Analysis of AS Aggregation in Cells. Image processing was performed with ImageJ (NIH, USA) and DIPimage toolbox for Matlab (TUDelft, Holland).

Statistics. The significance of the difference between means was evaluated with unpaired, two-tailed student's t-tests. In the live cell experiments, data are reported as means ± s.e.m., with sample set sizes $n > 10$ and $P < 0.05$.

Acknowledgment. E.A.J.-E. is funded by the Max Planck Society (Partner Group grant), ANPCyT, CONICET, and UBACyT. This work was supported by the DFG Center for Molecular Physiology of the Brain (DFG CMPB), Cluster of Excellence 171 of the CMPB, in Göttingen, Germany, and the Max Planck Society (Toxic Protein Conformation project). M.J.R. received fellowship support from the DFG CMPB and CONICET. M.M. received a doctoral fellowship from UBA. We are grateful to C. Bertoncini for suggestions, discussions, and assistance in the *in vitro* aggregation studies; N. Jonesheit for technical help; and S. Thirunavukkuarasu and the reviewers for valuable suggestions regarding the manuscript.

Supporting Information Available: Figures detailing the spectral properties of AS-C4-FlAsH and QDs, the imaging of AS-C4-FlAsH fibrils in the absence of QDs, ThioflavinT staining of fibrils formed *in vitro*, measurements of fibrils and QDs by AFM, blinking of QDs associated with aggregated AS-C4-FlAsH, and procedure for analyzing the kinetic traces of aggregation *in vitro* monitored by ThioflavinT. Supporting table with the quantitative analysis of aggregation in cells based on intensity and area calculations. Supporting movie depicting the blinking of QDs. Detailed description of AFM experiments. Details regarding the determination of the bAS loading factor m and of the QD streptavidin content s. Complete ref 25. This material is available free of charge via the Internet at http://pubs.acs.org.

JA900225W